Mon. Not. R. Astron. Soc. **272,** 41–48 (1995)

Recombination line intensities for hydrogenic ions – IV. Total recombination coefficients and machine-readable tables for $Z = 1$ to 8

P. J. Storey[1] and D. G. Hummer[2,3]

[1] *Department of Physics and Astronomy, University College London, Gower Street, London WC1E 6BT*
[2] *Max-Planck-Institut für Astrophysik, Postfach 1523, 85740 Garching bei München, Germany*
[3] *Institut für Astronomie und Astrophysik, Scheinerstrasse 1, 81679 München 80, Germany*

Accepted 1994 July 28. Received 1994 July 28; in original form 1993 August 20

ABSTRACT

Line emissivities, effective recombination coefficients, opacity factors, departure coefficients and total recombination coefficients are calculated for hydrogenic ions with $Z \leq 8$. Results are obtained for Cases A and B for $n \leq 50$. Collisional transitions among individual n and l states are fully treated. Calculations were made for log $N_e = 2(1)14$ for Case B and log $N_e = 2(1)10$ for Case A. The electron temperature takes between nine and 12 values, lying within the range 500 to 100 000 K, depending on the ion. All results are available in the form of machine-readable files.

Secondary files containing only effective emissivities for transitions for $n \leq 25$ and total recombination coefficients are also available for use with an interactive data server. The server produces tables of relative intensities of any two specified transitions or emissivities for any transition at all temperatures and densities in the data set. Extensive facilities for two-dimensional interpolation of relative intensities, emissivities and total recombination coefficients are provided.

Key words: atomic data – atomic processes – line: formation – astronomical data bases: miscellaneous.

1 INTRODUCTION

In two earlier papers (Hummer & Storey 1987; Storey & Hummer 1988; hereafter Papers I and II, respectively), we presented extensive calculations of the recombination spectra of hydrogenic ions in Case B of Baker & Menzel (1938) for nuclear charges $Z = 1$, 2, 6, 7 and 8. Since the appearance of Papers I and II, we have received numerous requests for machine-readable tables, for results for Case A and for other hydrogenic ions (because of their utility for hydrogenic transitions in complex ions), and for more detailed information, which it was not then feasible to publish because of space limitations.

Here we describe new calculations for all ions with $Z \leq 8$ with both Cases A and B, for which the results are available in machine-readable files. The same physical processes are included as in our earlier work; in particular, full account is taken of the individual l-states and of collisional processes.

The primary files contain emissivities for $n_u \rightarrow n_l$ transitions, effective recombination coefficients and departure coefficients $b(n, l)$ for (n, l) states, and $b(n)$ obtained by assuming that all l-distributions are thermal. As shown in Hummer & Storey (1992; hereafter Paper III), the $b(n)$ are not in general equal to the weighted sum of $b(n, l)$.

Line opacity factors for all transitions are also tabulated, which allow the optical thickness to be estimated if a geometrical scalelength is available. This is useful in applications to check that the transitions in question are indeed optically thin, as required by the theory. This condition may indeed not be satisfied for all objects with densities comparable to the higher values treated in this paper.

A set of secondary files containing the line emissivities for all transitions with $n \leq 25$ and total recombination coefficients is also provided for use with an interactive data server (INTRAT). This FORTRAN program gives a tabular display of the ratios of the intensities of two specified transitions, and the emissivities of any specified transition, for all temperatures and densities in the tables. A table of the total recombination coefficients can also be displayed. Extensive facilities are provided for two-dimensional interpolation in these tables.

In the next section, the physical and computational basis of this work is summarized. Section 3 describes tables of total recombination coefficients for Cases A and B. Section 4 describes the primary output files, and Section 5 deals with the secondary files and the use of the associated data server. Finally, conditions for the application of these results to hydrogenic and non-hydrogenic systems are discussed in Section 6.

2 CALCULATION OF $b(n, l)$

The calculation is carried out using the theory and atomic data described in Papers I and II. Further improvements to the computational method described in Paper III are also used here.

The calculation is made in two stages, the first being a calculation of $b(n)$, in which it is assumed that the populations of the l-substates are proportional to $(2l+1)$ for all n. In this calculation, as described in Papers I, II and III, the departure coefficients are interpolated using natural cubic splines in the variable $\varepsilon_n = 1/n^2$, where $b(\varepsilon = 0) = 1$. The penultimate point in the interpolation mesh must be chosen so that $b(\varepsilon_n)$ is close to unity. It was shown in Paper III that, for large n, $[1 - b(n)] \propto n^{-5}$, and an expression was given for the principal quantum number above which this form is valid (equation 3.10). We use this equation, with the constant modified, to choose automatically, for a particular temperature and density, the maximum principal quantum number, n_0, in the interpolation mesh.

$$n_0 = 240\eta^{-1/7}\theta^{1/14}, \tag{1}$$

where

$$\eta = N_e/Z^7 \quad \text{and} \quad \theta = T_e/Z^2. \tag{2}$$

In the second stage of the calculation, we must choose the value of n_c above which it can safely be assumed that the distribution of l-states is proportional to $(2l+1)$. This choice is also now made automatically according to the following algorithm. For the np states, the ratio r, of the total rate of radiative decay to the rate of collisional excitation from np to nd, is calculated. The probability of an l-increasing collision occurring is then approximately $p = 1/(1+r)$. We choose n_c to be the largest value of n for which $(1-p^n)$ is greater than 0.1. In other words, at $n = n_c$, there is approximately a 90 per cent chance that an atom will be transferred from the np state to the state with $l = n-1$ before a radiative decay can intervene. This turns out to be a very conservative requirement, in that, with this choice of n_c, the calculated departure coefficients $b(n_c, l)$ differ by no more than 1 per cent between $l = 0$ and $l = n-1$. An upper limit of $n_c = 245$ was set to keep the calculations within available computer resources. In some cases, at low electron densities and high nuclear charge, a larger value of n_c was required from the above algorithm. In cases where the tables show that the calculations were made with $n_c = 245$ (see Section 3), the computed departure coefficients should be treated with caution, particularly for the higher principal quantum numbers.

In the calculations described here, the ground state populations are not calculated, but instead are fixed at a sufficiently low value that collisional excitation from the ground state is negligible. In Case A, Lyα is defined to be optically thin; in Case B it is assumed to be optically thin, for, unless the Lyα optical depth is very large, the $n = 2$ population is so small that electron collisional excitations are negligible. This process cannot be included without parametrizing the problem in terms of the Lyα escape probability (cf. Paper I, section 4 and Paper II, section 4).

3 TOTAL RECOMBINATION COEFFICIENTS

The total recombination coefficients as functions of T_e and N_e are given in Tables 1 and 2 for Cases B and A, respectively. The principal trend in the tables is the transition from radiative recombination at low densities to three-body recombination at high densities, where the recombination coefficient increases linearly with electron density. The transition between the two types of recombination depends only on the reduced temperature and density, θ and η, defined above.

There is also a trend at low densities for the total recombination coefficients to be more sensitive to density at low temperatures. This results from the relatively large contribution of the large-n states, as these states are much more sensitive to collisions and thus to N_e than those with small values of n.

4 PRIMARY OUTPUT FILES

The primary output consists of a number of files labelled **rzctttt.d**, where **z** is the charge of the recombining ion, **c** is the Case identifier *a* or *b*, and **tttt** is $10^{-2}T_e$ written as an integer. Each Case B file contains data for 12 values of electron density, $\log N_e = 2(1)14$, and each Case A file holds data for nine values, $\log N_e = 2(1)10$. For each value of N_e, five types of data are given:

(1) Emissivities for transitions $(n_u \rightarrow n_l)$, $50 \geq n_u > n_l \geq 1$. The emissivity $\varepsilon(n_u \rightarrow n_l)$ is defined such that the energy emitted in the $(n_u \rightarrow n_l)$ transition per unit time per unit volume is $N_e N_+ \varepsilon(n_u \rightarrow n_l)$ (erg s^{-1} cm^{-3}).

(2) Effective recombination coefficients to levels (n, l). The effective recombination coefficient $\overline{\alpha}(n, l)$ (cm^3 s^{-1}) includes the effects of radiative and three-body recombination and radiative cascading, and expresses the rate per unit volume per unit electron and unit ion densities at which the level (n, l) is populated by states of different n.

(3) Line opacity factors for all transitions $(1 \leq n_l < n_u \leq 50)$. The quantities tabulated are $\Omega_{n_l, n_u} \times 10^{20}$, where Ω_{n_l, n_u} is defined in Paper I, equation (29). The factor of 10^{20} has been introduced to cope with numerical problems in the calculation. The mean optical thickness in the transition is obtained by multiplying Ω_{n_l, n_u} by the thickness, in cm, of the emitting region.

(4) Departure coefficients $b(n, l)$. This is the ratio of the actual population of the level (n, l) to its value in thermal equilibrium, with the same ion and electron densities.

(5) Departure coefficients $b(n)$ calculated with the assumption of a thermal l-distribution. This quantity is the ratio of the population of level n, calculated with the assumption that the l-levels are proportional to $(2l+1)$, to the value in thermal equilibrium.

The files are designed to be read with either an interactive editor or an applications program. The structure of the files can be seen in Fig. 1, where a cut-down version of the data for the first density of file **r1b0100.d** is reproduced. For practicability, most of the data has had to be omitted at places indicated by dotted lines, but the structure of the file should be clear. For each density, the first line indicates the physical parameters and the parameter n_c, with the numerical values given directly below (for convenience in use with

Table 1. Total recombination coefficients, α_B ($cm^3\ s^{-1}$), for hydrogenic ions.

Z	T(K)	Ne=	1.000E+02	1.000E+03	1.000E+04	1.000E+05	1.000E+06	1.000E+07	1.000E+08	1.000E+09	1.000E+10	1.000E+11	1.000E+12	1.000E+13	1.000E+14
1	5.000E+02		2.493E-12	2.573E-12	2.720E-12	2.998E-12	3.542E-12	4.681E-12	7.330E-12	1.462E-11	4.044E-11	1.700E-10	1.119E-09	9.959E-09	9.756E-08
	1.000E+03		1.512E-12	1.535E-12	1.579E-12	1.658E-12	1.810E-12	2.106E-12	2.717E-12	4.111E-12	7.823E-12	2.037E-11	7.981E-11	4.937E-10	4.266E-09
	3.000E+03		6.708E-13	6.740E-13	6.798E-13	6.907E-13	7.109E-13	7.486E-13	8.204E-13	9.615E-13	1.257E-12	1.941E-12	3.811E-12	1.040E-11	4.325E-11
	5.000E+03		4.522E-13	4.534E-13	4.556E-13	4.597E-13	4.674E-13	4.816E-13	5.083E-13	5.592E-13	6.601E-13	8.726E-13	1.371E-12	2.755E-12	7.792E-12
	7.500E+03		3.273E-13	3.278E-13	3.288E-13	3.306E-13	3.341E-13	3.404E-13	3.524E-13	3.749E-13	4.181E-13	5.047E-13	6.908E-13	1.138E-12	2.453E-12
	1.000E+04		2.585E-13	2.588E-13	2.594E-13	2.604E-13	2.623E-13	2.658E-13	2.724E-13	2.848E-13	3.083E-13	3.541E-13	4.477E-13	6.551E-13	1.200E-12
	1.250E+04		2.144E-13	2.147E-13	2.149E-13	2.156E-13	2.167E-13	2.190E-13	2.230E-13	2.307E-13	2.452E-13	2.728E-13	3.276E-13	4.426E-13	7.303E-13
	1.500E+04		1.836E-13	1.837E-13	1.839E-13	1.843E-13	1.851E-13	1.866E-13	1.893E-13	1.944E-13	2.040E-13	2.221E-13	2.571E-13	3.278E-13	5.036E-13
	2.000E+04		1.428E-13	1.429E-13	1.430E-13	1.432E-13	1.436E-13	1.444E-13	1.458E-13	1.484E-13	1.532E-13	1.621E-13	1.788E-13	2.106E-13	2.959E-13
	3.000E+04		9.911E-14	9.913E-14	9.917E-14	9.924E-14	9.937E-14	9.962E-14	1.001E-13	1.009E-13	1.025E-13	1.054E-13	1.103E-13	1.190E-13	1.528E-13
2	5.000E+02		1.262E-11	1.314E-11	1.412E-11	1.600E-11	1.982E-11	2.824E-11	4.989E-11	1.199E-10	4.344E-10	2.507E-09	2.081E-08	1.996E-07	1.931E-06
	1.000E+03		7.826E-12	7.984E-12	8.277E-12	8.828E-12	9.886E-12	1.200E-11	1.662E-11	2.813E-11	6.381E-11	2.151E-10	1.157E-09	9.213E-09	8.764E-08
	3.000E+03		3.657E-12	3.680E-12	3.723E-12	3.802E-12	3.950E-12	4.229E-12	4.771E-12	5.872E-12	8.315E-12	1.459E-11	3.491E-11	1.266E-10	7.362E-10
	5.000E+03		2.545E-12	2.554E-12	2.571E-12	2.602E-12	2.661E-12	2.772E-12	2.981E-12	3.391E-12	4.233E-12	6.131E-12	1.114E-11	2.802E-11	1.085E-10
	7.500E+03		1.897E-12	1.900E-12	1.909E-12	1.923E-12	1.952E-12	2.004E-12	2.103E-12	2.293E-12	2.668E-12	3.458E-12	5.313E-12	1.054E-11	3.000E-11
	1.000E+04		1.533E-12	1.536E-12	1.541E-12	1.549E-12	1.566E-12	1.596E-12	1.654E-12	1.764E-12	1.978E-12	2.412E-12	3.371E-12	5.817E-12	1.365E-11
	1.250E+04		1.297E-12	1.298E-12	1.301E-12	1.307E-12	1.318E-12	1.338E-12	1.376E-12	1.448E-12	1.586E-12	1.862E-12	2.447E-12	3.849E-12	7.914E-12
	1.500E+04		1.128E-12	1.129E-12	1.132E-12	1.136E-12	1.143E-12	1.157E-12	1.184E-12	1.235E-12	1.332E-12	1.523E-12	1.917E-12	2.822E-12	5.263E-12
	2.000E+04		9.030E-13	9.035E-13	9.048E-13	9.071E-13	9.115E-13	9.197E-13	9.351E-13	9.641E-13	1.019E-12	1.126E-12	1.340E-12	1.803E-12	2.941E-12
	3.000E+04		6.540E-13	6.543E-13	6.548E-13	6.558E-13	6.578E-13	6.615E-13	6.683E-13	6.813E-13	7.058E-13	7.524E-13	8.432E-13	1.029E-12	1.440E-12
	5.000E+04		4.288E-13	4.289E-13	4.290E-13	4.294E-13	4.300E-13	4.313E-13	4.336E-13	4.381E-13	4.464E-13	4.622E-13	4.922E-13	5.505E-13	6.683E-13
	1.000E+05		2.341E-13	2.341E-13	2.341E-13	2.342E-13	2.343E-13	2.346E-13	2.350E-13	2.358E-13	2.375E-13	2.404E-13	2.459E-13	2.561E-13	2.746E-13
3	1.000E+03		1.998E-11	2.043E-11	2.130E-11	2.295E-11	2.616E-11	3.278E-11	4.777E-11	8.789E-11	2.263E-10	9.055E-10	5.775E-09	5.055E-08	4.879E-07
	3.000E+03		9.549E-12	9.615E-12	9.742E-12	9.981E-12	1.043E-11	1.130E-11	1.299E-11	1.653E-11	2.475E-11	4.752E-11	1.303E-10	5.633E-10	3.849E-09
	5.000E+03		6.733E-12	6.760E-12	6.811E-12	6.908E-12	7.089E-12	7.434E-12	8.093E-12	9.400E-12	1.217E-11	1.873E-11	3.750E-11	1.090E-10	5.059E-10
	7.500E+03		5.079E-12	5.091E-12	5.115E-12	5.162E-12	5.250E-12	5.416E-12	5.730E-12	6.338E-12	7.567E-12	1.025E-11	1.693E-11	3.762E-11	1.259E-10
	1.000E+04		4.145E-12	4.152E-12	4.167E-12	4.194E-12	4.246E-12	4.344E-12	4.531E-12	4.887E-12	5.589E-12	7.056E-12	1.045E-11	1.982E-11	5.357E-11
	1.250E+04		3.534E-12	3.537E-12	3.548E-12	3.566E-12	3.601E-12	3.666E-12	3.790E-12	4.024E-12	4.483E-12	5.416E-12	7.479E-12	1.275E-11	2.969E-11
	1.500E+04		3.097E-12	3.100E-12	3.107E-12	3.120E-12	3.145E-12	3.192E-12	3.280E-12	3.448E-12	3.771E-12	4.419E-12	5.809E-12	9.176E-12	1.915E-11
	2.000E+04		2.508E-12	2.509E-12	2.514E-12	2.522E-12	2.536E-12	2.564E-12	2.615E-12	2.713E-12	2.900E-12	3.268E-12	4.026E-12	5.743E-12	1.030E-11
	3.000E+04		1.851E-12	1.851E-12	1.854E-12	1.857E-12	1.863E-12	1.877E-12	1.901E-12	1.946E-12	2.033E-12	2.199E-12	2.530E-12	3.228E-12	4.872E-12
	5.000E+04		1.247E-12	1.247E-12	1.247E-12	1.249E-12	1.251E-12	1.256E-12	1.265E-12	1.282E-12	1.314E-12	1.375E-12	1.492E-12	1.727E-12	2.227E-12
	1.000E+05		7.101E-13	7.101E-13	7.104E-13	7.107E-13	7.113E-13	7.124E-13	7.145E-13	7.185E-13	7.262E-13	7.408E-13	7.685E-13	8.216E-13	9.263E-13
4	3.000E+03		1.866E-11	1.878E-11	1.905E-11	1.958E-11	2.055E-11	2.244E-11	2.622E-11	3.425E-11	5.361E-11	1.105E-10	3.364E-10	1.647E-09	1.238E-08
	5.000E+03		1.326E-11	1.331E-11	1.342E-11	1.363E-11	1.403E-11	1.478E-11	1.624E-11	1.918E-11	2.555E-11	4.125E-11	8.912E-11	2.890E-10	1.518E-09
	7.500E+03		1.007E-11	1.010E-11	1.015E-11	1.025E-11	1.044E-11	1.081E-11	1.151E-11	1.287E-11	1.568E-11	2.196E-11	3.836E-11	9.308E-11	3.508E-10
	1.000E+04		8.264E-12	8.278E-12	8.310E-12	8.370E-12	8.485E-12	8.703E-12	9.118E-12	9.918E-12	1.152E-11	1.493E-11	2.313E-11	4.712E-11	1.416E-10
	1.250E+04		7.077E-12	7.086E-12	7.107E-12	7.148E-12	7.225E-12	7.370E-12	7.648E-12	8.176E-12	9.220E-12	1.138E-11	1.631E-11	2.957E-11	7.564E-11
	1.500E+04		6.228E-12	6.234E-12	6.249E-12	6.277E-12	6.334E-12	6.437E-12	6.637E-12	7.016E-12	7.753E-12	9.255E-12	1.256E-11	2.093E-11	4.749E-11
	2.000E+04		5.078E-12	5.082E-12	5.090E-12	5.107E-12	5.140E-12	5.202E-12	5.320E-12	5.543E-12	5.972E-12	6.825E-12	8.624E-12	1.284E-11	2.465E-11
	3.000E+04		3.788E-12	3.789E-12	3.793E-12	3.801E-12	3.816E-12	3.846E-12	3.902E-12	4.007E-12	4.207E-12	4.598E-12	5.384E-12	7.086E-12	1.126E-11
	5.000E+04		2.590E-12	2.592E-12	2.593E-12	2.596E-12	2.602E-12	2.613E-12	2.634E-12	2.674E-12	2.751E-12	2.897E-12	3.182E-12	3.761E-12	5.030E-12
	1.000E+05		1.514E-12	1.514E-12	1.514E-12	1.515E-12	1.516E-12	1.519E-12	1.524E-12	1.535E-12	1.555E-12	1.592E-12	1.664E-12	1.804E-12	2.083E-12

Table 1 – *continued*

Z	T(K)	Ne=	1.000E+02	1.000E+03	1.000E+04	1.000E+05	1.000E+06	1.000E+07	1.000E+08	1.000E+09	1.000E+10	1.000E+11	1.000E+12	1.000E+13	1.000E+14
5	3.000E+03		3.119E-11	3.141E-11	3.187E-11	3.280E-11	3.459E-11	3.803E-11	4.500E-11	6.016E-11	9.774E-11	2.140E-10	7.080E-10	3.807E-09	3.047E-08
	5.000E+03		2.229E-11	2.238E-11	2.257E-11	2.294E-11	2.366E-11	2.504E-11	2.773E-11	3.321E-11	4.529E-11	7.612E-11	1.752E-10	6.202E-10	3.568E-09
	7.500E+03		1.701E-11	1.705E-11	1.714E-11	1.732E-11	1.767E-11	1.835E-11	1.963E-11	2.217E-11	2.743E-11	3.954E-11	7.241E-11	1.888E-10	7.802E-10
	1.000E+04		1.401E-11	1.404E-11	1.409E-11	1.420E-11	1.441E-11	1.481E-11	1.557E-11	1.706E-11	2.005E-11	2.657E-11	4.274E-11	9.238E-11	3.021E-10
	1.250E+04		1.203E-11	1.205E-11	1.209E-11	1.216E-11	1.230E-11	1.257E-11	1.308E-11	1.407E-11	1.602E-11	2.013E-11	2.976E-11	5.672E-11	1.566E-10
	1.500E+04		1.062E-11	1.063E-11	1.065E-11	1.071E-11	1.081E-11	1.100E-11	1.137E-11	1.208E-11	1.346E-11	1.631E-11	2.272E-11	3.956E-11	9.611E-11
	2.000E+04		8.697E-12	8.703E-12	8.718E-12	8.750E-12	8.809E-12	8.924E-12	9.142E-12	9.561E-12	1.037E-11	1.198E-11	1.545E-11	2.381E-11	4.839E-11
	3.000E+04		6.534E-12	6.536E-12	6.543E-12	6.557E-12	6.586E-12	6.641E-12	6.745E-12	6.944E-12	7.323E-12	8.065E-12	9.579E-12	1.292E-11	2.141E-11
	5.000E+04		4.515E-12	4.516E-12	4.519E-12	4.524E-12	4.535E-12	4.557E-12	4.597E-12	4.675E-12	4.820E-12	5.102E-12	5.655E-12	6.791E-12	9.337E-12
	1.000E+05		2.683E-12	2.683E-12	2.684E-12	2.685E-12	2.688E-12	2.694E-12	2.704E-12	2.725E-12	2.764E-12	2.839E-12	2.982E-12	3.262E-12	3.831E-12
6	3.000E+03		4.731E-11	4.766E-11	4.838E-11	4.983E-11	5.270E-11	5.833E-11	6.974E-11	9.513E-11	1.598E-10	3.686E-10	1.308E-09	7.565E-09	6.320E-08
	5.000E+03		3.395E-11	3.408E-11	3.437E-11	3.496E-11	3.613E-11	3.838E-11	4.277E-11	5.186E-11	7.223E-11	1.257E-10	3.053E-10	1.162E-09	7.177E-09
	7.500E+03		2.600E-11	2.607E-11	2.620E-11	2.649E-11	2.706E-11	2.815E-11	3.025E-11	3.445E-11	4.325E-11	6.387E-11	1.218E-10	3.373E-10	1.503E-09
	1.000E+04		2.147E-11	2.151E-11	2.159E-11	2.177E-11	2.211E-11	2.276E-11	2.401E-11	2.646E-11	3.145E-11	4.247E-11	7.051E-11	1.604E-10	5.629E-10
	1.250E+04		1.849E-11	1.851E-11	1.857E-11	1.868E-11	1.891E-11	1.935E-11	2.018E-11	2.181E-11	2.506E-11	3.198E-11	4.853E-11	9.660E-11	2.843E-10
	1.500E+04		1.634E-11	1.636E-11	1.640E-11	1.648E-11	1.665E-11	1.697E-11	1.757E-11	1.873E-11	2.103E-11	2.581E-11	3.679E-11	6.649E-11	1.712E-10
	2.000E+04		1.343E-11	1.344E-11	1.346E-11	1.351E-11	1.361E-11	1.380E-11	1.416E-11	1.485E-11	1.619E-11	1.890E-11	2.479E-11	3.935E-11	8.389E-11
	3.000E+04		1.014E-11	1.015E-11	1.016E-11	1.018E-11	1.023E-11	1.032E-11	1.049E-11	1.082E-11	1.145E-11	1.269E-11	1.526E-11	2.102E-11	3.606E-11
	5.000E+04		7.061E-12	7.062E-12	7.066E-12	7.074E-12	7.092E-12	7.127E-12	7.196E-12	7.325E-12	7.572E-12	8.045E-12	8.982E-12	1.093E-11	1.538E-11
	1.000E+05		4.246E-12	4.247E-12	4.248E-12	4.250E-12	4.255E-12	4.264E-12	4.282E-12	4.317E-12	4.385E-12	4.513E-12	4.760E-12	5.244E-12	6.240E-12
7	5.000E+03		4.834E-11	4.854E-11	4.894E-11	4.981E-11	5.154E-11	5.492E-11	6.158E-11	7.542E-11	1.071E-10	1.923E-10	4.899E-10	1.982E-09	1.294E-08
	7.500E+03		3.713E-11	3.722E-11	3.742E-11	3.784E-11	3.869E-11	4.032E-11	4.350E-11	4.987E-11	6.344E-11	9.575E-11	1.892E-10	5.524E-10	2.623E-09
	1.000E+04		3.073E-11	3.078E-11	3.090E-11	3.116E-11	3.166E-11	3.264E-11	3.454E-11	3.825E-11	4.593E-11	6.305E-11	1.077E-10	2.561E-10	9.544E-10
	1.250E+04		2.651E-11	2.654E-11	2.661E-11	2.679E-11	2.712E-11	2.779E-11	2.906E-11	3.152E-11	3.650E-11	4.721E-11	7.335E-11	1.517E-10	4.716E-10
	1.500E+04		2.347E-11	2.349E-11	2.355E-11	2.367E-11	2.391E-11	2.439E-11	2.530E-11	2.707E-11	3.059E-11	3.798E-11	5.521E-11	1.031E-10	2.792E-10
	2.000E+04		1.934E-11	1.935E-11	1.938E-11	1.945E-11	1.960E-11	1.988E-11	2.043E-11	2.147E-11	2.353E-11	2.770E-11	3.690E-11	6.012E-11	1.336E-10
	3.000E+04		1.466E-11	1.466E-11	1.468E-11	1.471E-11	1.478E-11	1.492E-11	1.518E-11	1.568E-11	1.666E-11	1.856E-11	2.255E-11	3.162E-11	5.596E-11
	5.000E+04		1.026E-11	1.026E-11	1.027E-11	1.028E-11	1.031E-11	1.036E-11	1.047E-11	1.066E-11	1.104E-11	1.177E-11	1.323E-11	1.629E-11	2.338E-11
	1.000E+05		6.228E-12	6.228E-12	6.230E-12	6.233E-12	6.240E-12	6.254E-12	6.283E-12	6.338E-12	6.443E-12	6.643E-12	7.030E-12	7.793E-12	9.375E-12
8	5.000E+03		6.556E-11	6.582E-11	6.639E-11	6.757E-11	6.998E-11	7.478E-11	8.428E-11	1.042E-10	1.506E-10	2.780E-10	7.401E-10	3.154E-09	2.155E-08
	7.500E+03		5.048E-11	5.059E-11	5.087E-11	5.144E-11	5.262E-11	5.495E-11	5.948E-11	6.862E-11	8.830E-11	1.360E-10	2.776E-10	8.485E-10	4.249E-09
	1.000E+04		4.185E-11	4.191E-11	4.208E-11	4.242E-11	4.312E-11	4.452E-11	4.722E-11	5.256E-11	6.363E-11	8.872E-11	1.554E-10	3.845E-10	1.510E-09
	1.250E+04		3.615E-11	3.619E-11	3.629E-11	3.652E-11	3.700E-11	3.794E-11	3.975E-11	4.328E-11	5.046E-11	6.609E-11	1.049E-10	2.242E-10	7.320E-10
	1.500E+04		3.204E-11	3.208E-11	3.215E-11	3.231E-11	3.265E-11	3.333E-11	3.464E-11	3.717E-11	4.224E-11	5.299E-11	7.841E-11	1.509E-10	4.270E-10
	2.000E+04		2.645E-11	2.647E-11	2.651E-11	2.660E-11	2.681E-11	2.721E-11	2.799E-11	2.950E-11	3.245E-11	3.851E-11	5.201E-11	8.674E-11	2.001E-10
	3.000E+04		2.010E-11	2.012E-11	2.014E-11	2.018E-11	2.028E-11	2.048E-11	2.085E-11	2.158E-11	2.297E-11	2.575E-11	3.156E-11	4.500E-11	8.184E-11
	5.000E+04		1.415E-11	1.415E-11	1.415E-11	1.417E-11	1.421E-11	1.429E-11	1.443E-11	1.472E-11	1.527E-11	1.633E-11	1.846E-11	2.295E-11	3.353E-11
	1.000E+05		8.647E-12	8.648E-12	8.650E-12	8.654E-12	8.664E-12	8.685E-12	8.727E-12	8.806E-12	8.960E-12	9.253E-12	9.819E-12	1.094E-11	1.329E-11

Table 2. Total recombination coefficients, α_A ($cm^3\ s^{-1}$), for hydrogenic ions.

Z	T(K)	Ne=	1.000E+02	1.000E+03	1.000E+04	1.000E+05	1.000E+06	1.000E+07	1.000E+08	1.000E+09	1.000E+10
1	5.000E+02		3.251E-12	3.351E-12	3.536E-12	3.880E-12	4.552E-12	5.943E-12	9.129E-12	1.769E-11	4.694E-11
	1.000E+03		2.038E-12	2.069E-12	2.125E-12	2.229E-12	2.424E-12	2.802E-12	3.575E-12	5.308E-12	9.817E-12
	3.000E+03		9.690E-13	9.735E-13	9.819E-13	9.973E-13	1.026E-12	1.079E-12	1.179E-12	1.374E-12	1.778E-12
	5.000E+03		6.809E-13	6.827E-13	6.861E-13	6.923E-13	7.038E-13	7.252E-13	7.651E-13	8.406E-13	9.890E-13
	7.500E+03		5.120E-13	5.128E-13	5.145E-13	5.174E-13	5.230E-13	5.333E-13	5.524E-13	5.883E-13	6.569E-13
	1.000E+04		4.169E-13	4.174E-13	4.183E-13	4.201E-13	4.234E-13	4.294E-13	4.408E-13	4.619E-13	5.018E-13
	1.250E+04		3.547E-13	3.550E-13	3.557E-13	3.568E-13	3.590E-13	3.630E-13	3.705E-13	3.844E-13	4.107E-13
	1.500E+04		3.104E-13	3.106E-13	3.111E-13	3.119E-13	3.134E-13	3.163E-13	3.216E-13	3.315E-13	3.501E-13
	2.000E+04		2.507E-13	2.509E-13	2.511E-13	2.516E-13	2.525E-13	2.541E-13	2.572E-13	2.630E-13	2.737E-13
	3.000E+04		1.843E-13	1.844E-13	1.845E-13	1.847E-13	1.851E-13	1.858E-13	1.872E-13	1.898E-13	1.947E-13
2	5.000E+02		1.568E-11	1.630E-11	1.747E-11	1.970E-11	2.418E-11	3.396E-11	5.865E-11	1.363E-10	4.727E-10
	1.000E+03		9.945E-12	1.014E-11	1.049E-11	1.116E-11	1.244E-11	1.498E-11	2.045E-11	3.385E-11	7.423E-11
	3.000E+03		4.863E-12	4.892E-12	4.946E-12	5.047E-12	5.236E-12	5.590E-12	6.273E-12	7.649E-12	1.066E-11
	5.000E+03		3.475E-12	3.486E-12	3.508E-12	3.550E-12	3.628E-12	3.773E-12	4.047E-12	4.577E-12	5.656E-12
	7.500E+03		2.653E-12	2.658E-12	2.669E-12	2.690E-12	2.728E-12	2.799E-12	2.932E-12	3.186E-12	3.684E-12
	1.000E+04		2.186E-12	2.189E-12	2.196E-12	2.208E-12	2.231E-12	2.274E-12	2.354E-12	2.505E-12	2.797E-12
	1.250E+04		1.879E-12	1.881E-12	1.885E-12	1.893E-12	1.909E-12	1.938E-12	1.992E-12	2.093E-12	2.287E-12
	1.500E+04		1.658E-12	1.660E-12	1.663E-12	1.669E-12	1.680E-12	1.701E-12	1.740E-12	1.813E-12	1.952E-12
	2.000E+04		1.359E-12	1.360E-12	1.362E-12	1.366E-12	1.372E-12	1.385E-12	1.408E-12	1.452E-12	1.534E-12
	3.000E+04		1.023E-12	1.023E-12	1.024E-12	1.026E-12	1.029E-12	1.035E-12	1.046E-12	1.067E-12	1.106E-12
	5.000E+04		7.092E-13	7.093E-13	7.097E-13	7.103E-13	7.115E-13	7.138E-13	7.181E-13	7.262E-13	7.415E-13
	1.000E+05		4.238E-13	4.238E-13	4.239E-13	4.241E-13	4.244E-13	4.250E-13	4.261E-13	4.282E-13	4.323E-13
3	1.000E+03		2.476E-11	2.529E-11	2.633E-11	2.828E-11	3.206E-11	3.980E-11	5.710E-11	1.025E-10	2.546E-10
	3.000E+03		1.227E-11	1.235E-11	1.250E-11	1.280E-11	1.335E-11	1.441E-11	1.647E-11	2.073E-11	3.047E-11
	5.000E+03		8.831E-12	8.864E-12	8.928E-12	9.050E-12	9.279E-12	9.711E-12	1.053E-11	1.215E-11	1.554E-11
	7.500E+03		6.788E-12	6.803E-12	6.835E-12	6.895E-12	7.008E-12	7.221E-12	7.622E-12	8.394E-12	9.940E-12
	1.000E+04		5.622E-12	5.631E-12	5.650E-12	5.687E-12	5.755E-12	5.884E-12	6.125E-12	6.586E-12	7.488E-12
	1.250E+04		4.852E-12	4.859E-12	4.871E-12	4.896E-12	4.942E-12	5.029E-12	5.192E-12	5.501E-12	6.099E-12
	1.500E+04		4.299E-12	4.304E-12	4.313E-12	4.331E-12	4.364E-12	4.427E-12	4.546E-12	4.769E-12	5.198E-12
	2.000E+04		3.547E-12	3.549E-12	3.555E-12	3.565E-12	3.585E-12	3.623E-12	3.695E-12	3.828E-12	4.083E-12
	3.000E+04		2.695E-12	2.696E-12	2.699E-12	2.704E-12	2.714E-12	2.732E-12	2.767E-12	2.831E-12	2.954E-12
	5.000E+04		1.894E-12	1.895E-12	1.896E-12	1.898E-12	1.902E-12	1.909E-12	1.923E-12	1.949E-12	1.997E-12
	1.000E+05		1.159E-12	1.159E-12	1.159E-12	1.159E-12	1.160E-12	1.162E-12	1.166E-12	1.173E-12	1.187E-12
4	3.000E+03		2.349E-11	2.365E-11	2.397E-11	2.460E-11	2.578E-11	2.804E-11	3.254E-11	4.200E-11	6.447E-11
	5.000E+03		1.699E-11	1.706E-11	1.719E-11	1.745E-11	1.793E-11	1.886E-11	2.064E-11	2.419E-11	3.179E-11
	7.500E+03		1.311E-11	1.314E-11	1.321E-11	1.334E-11	1.358E-11	1.403E-11	1.490E-11	1.658E-11	2.001E-11
	1.000E+04		1.090E-11	1.091E-11	1.095E-11	1.103E-11	1.118E-11	1.145E-11	1.197E-11	1.298E-11	1.496E-11
	1.250E+04		9.429E-12	9.441E-12	9.467E-12	9.519E-12	9.617E-12	9.804E-12	1.016E-11	1.083E-11	1.214E-11
	1.500E+04		8.373E-12	8.381E-12	8.400E-12	8.437E-12	8.509E-12	8.645E-12	8.902E-12	9.388E-12	1.033E-11
	2.000E+04		6.932E-12	6.937E-12	6.948E-12	6.971E-12	7.014E-12	7.096E-12	7.251E-12	7.543E-12	8.102E-12
	3.000E+04		5.297E-12	5.300E-12	5.305E-12	5.316E-12	5.337E-12	5.377E-12	5.453E-12	5.595E-12	5.865E-12
	5.000E+04		3.754E-12	3.755E-12	3.757E-12	3.761E-12	3.770E-12	3.786E-12	3.816E-12	3.873E-12	3.982E-12
	1.000E+05		2.326E-12	2.326E-12	2.327E-12	2.328E-12	2.330E-12	2.335E-12	2.343E-12	2.360E-12	2.390E-12
5	3.000E+03		3.876E-11	3.903E-11	3.957E-11	4.067E-11	4.278E-11	4.686E-11	5.504E-11	7.268E-11	1.156E-10
	5.000E+03		2.813E-11	2.824E-11	2.846E-11	2.891E-11	2.978E-11	3.144E-11	3.467E-11	4.119E-11	5.538E-11
	7.500E+03		2.177E-11	2.182E-11	2.193E-11	2.215E-11	2.258E-11	2.340E-11	2.497E-11	2.805E-11	3.436E-11
	1.000E+04		1.813E-11	1.816E-11	1.822E-11	1.836E-11	1.862E-11	1.911E-11	2.006E-11	2.189E-11	2.553E-11
	1.250E+04		1.572E-11	1.573E-11	1.578E-11	1.587E-11	1.605E-11	1.638E-11	1.702E-11	1.825E-11	2.065E-11
	1.500E+04		1.398E-11	1.399E-11	1.402E-11	1.409E-11	1.422E-11	1.446E-11	1.492E-11	1.581E-11	1.753E-11
	2.000E+04		1.160E-11	1.161E-11	1.163E-11	1.167E-11	1.174E-11	1.189E-11	1.217E-11	1.270E-11	1.372E-11
	3.000E+04		8.900E-12	8.903E-12	8.912E-12	8.931E-12	8.968E-12	9.041E-12	9.178E-12	9.438E-12	9.931E-12
	5.000E+04		6.341E-12	6.343E-12	6.346E-12	6.353E-12	6.368E-12	6.398E-12	6.453E-12	6.559E-12	6.757E-12
	1.000E+05		3.963E-12	3.964E-12	3.965E-12	3.967E-12	3.971E-12	3.979E-12	3.995E-12	4.025E-12	4.083E-12
6	3.000E+03		5.823E-11	5.864E-11	5.947E-11	6.118E-11	6.456E-11	7.113E-11	8.441E-11	1.136E-10	1.868E-10
	5.000E+03		4.237E-11	4.253E-11	4.287E-11	4.358E-11	4.497E-11	4.764E-11	5.284E-11	6.353E-11	8.719E-11
	7.500E+03		3.286E-11	3.294E-11	3.310E-11	3.345E-11	3.414E-11	3.545E-11	3.798E-11	4.299E-11	5.342E-11
	1.000E+04		2.741E-11	2.746E-11	2.755E-11	2.776E-11	2.818E-11	2.897E-11	3.050E-11	3.347E-11	3.946E-11
	1.250E+04		2.379E-11	2.382E-11	2.389E-11	2.403E-11	2.431E-11	2.485E-11	2.588E-11	2.787E-11	3.181E-11
	1.500E+04		2.118E-11	2.121E-11	2.125E-11	2.135E-11	2.156E-11	2.195E-11	2.270E-11	2.413E-11	2.695E-11
	2.000E+04		1.762E-11	1.763E-11	1.766E-11	1.772E-11	1.784E-11	1.808E-11	1.853E-11	1.939E-11	2.106E-11
	3.000E+04		1.355E-11	1.356E-11	1.357E-11	1.360E-11	1.366E-11	1.378E-11	1.400E-11	1.442E-11	1.523E-11
	5.000E+04		9.697E-12	9.699E-12	9.704E-12	9.715E-12	9.739E-12	9.786E-12	9.876E-12	1.005E-11	1.037E-11
	1.000E+05		6.099E-12	6.100E-12	6.101E-12	6.104E-12	6.111E-12	6.124E-12	6.150E-12	6.200E-12	6.295E-12
7	5.000E+03		5.982E-11	6.005E-11	6.054E-11	6.155E-11	6.359E-11	6.758E-11	7.539E-11	9.151E-11	1.280E-10
	7.500E+03		4.648E-11	4.659E-11	4.682E-11	4.732E-11	4.833E-11	5.029E-11	5.407E-11	6.160E-11	7.753E-11
	1.000E+04		3.882E-11	3.888E-11	3.902E-11	3.932E-11	3.993E-11	4.112E-11	4.339E-11	4.785E-11	5.697E-11
	1.250E+04		3.373E-11	3.378E-11	3.387E-11	3.407E-11	3.448E-11	3.528E-11	3.682E-11	3.980E-11	4.579E-11
	1.500E+04		3.006E-11	3.009E-11	3.016E-11	3.030E-11	3.060E-11	3.119E-11	3.230E-11	3.446E-11	3.873E-11
	2.000E+04		2.504E-11	2.505E-11	2.509E-11	2.518E-11	2.536E-11	2.571E-11	2.639E-11	2.768E-11	3.021E-11
	3.000E+04		1.930E-11	1.931E-11	1.933E-11	1.937E-11	1.946E-11	1.963E-11	1.996E-11	2.060E-11	2.182E-11
	5.000E+04		1.385E-11	1.386E-11	1.386E-11	1.388E-11	1.392E-11	1.399E-11	1.412E-11	1.438E-11	1.487E-11
	1.000E+05		8.758E-12	8.759E-12	8.760E-12	8.765E-12	8.774E-12	8.794E-12	8.834E-12	8.909E-12	9.053E-12
8	5.000E+03		8.057E-11	8.087E-11	8.155E-11	8.291E-11	8.574E-11	9.135E-11	1.024E-10	1.255E-10	1.783E-10
	7.500E+03		6.270E-11	6.284E-11	6.316E-11	6.383E-11	6.522E-11	6.799E-11	7.334E-11	8.406E-11	1.070E-10
	1.000E+04		5.242E-11	5.250E-11	5.269E-11	5.309E-11	5.394E-11	5.561E-11	5.882E-11	6.516E-11	7.820E-11
	1.250E+04		4.559E-11	4.565E-11	4.577E-11	4.604E-11	4.661E-11	4.774E-11	4.992E-11	5.415E-11	6.269E-11
	1.500E+04		4.066E-11	4.070E-11	4.079E-11	4.098E-11	4.139E-11	4.222E-11	4.379E-11	4.685E-11	5.294E-11
	2.000E+04		3.390E-11	3.393E-11	3.398E-11	3.409E-11	3.434E-11	3.484E-11	3.579E-11	3.763E-11	4.122E-11
	3.000E+04		2.619E-11	2.620E-11	2.622E-11	2.628E-11	2.640E-11	2.664E-11	2.711E-11	2.801E-11	2.974E-11
	5.000E+04		1.884E-11	1.885E-11	1.886E-11	1.888E-11	1.893E-11	1.902E-11	1.922E-11	1.958E-11	2.028E-11
	1.000E+05		1.196E-11	1.196E-11	1.196E-11	1.197E-11	1.198E-11	1.201E-11	1.206E-11	1.217E-11	1.238E-11

```
DENS          Z      TEMP            CASE    NMIN    NC
1.000E+02     1      1.000E+04       B       2       139
E_NU=50                 Z= 1  TE= 1.000E+04  NE= 1.000E+02  CASE=B
  1 0.000E+00   2 7.285E-29   3 2.319E-29   4 1.037E-29   5 5.559E-30   6 3.340E-30
  7 2.169E-30   8 1.491E-30   9 1.070E-30 10 7.946E-31 11 6.067E-31 12 4.738E-31
.....................................................................

 43 1.128E-32 44 1.046E-32 45 9.698E-33 46 8.964E-33 47 8.233E-33 48 7.441E-33
 49 6.333E-33
E_NU=49                 Z= 1  TE= 1.000E+04  NE= 1.000E+02  CASE=B
  1 0.000E+00   2 7.617E-29   3 2.431E-29   4 1.090E-29   5 5.863E-30   6 3.530E-30
.....................................................................

E_NU= 3                 Z= 1  TE= 1.000E+04  NE= 1.000E+02  CASE=B
  1 0.000E+00   2 3.536E-25
E_NU= 2                 Z= 1  TE= 1.000E+04  NE= 1.000E+02  CASE=B
  1 2.910E-24
R_NU=50                 Z= 1  TE= 1.000E+04  NE= 1.000E+02  CASE=B
  0 2.647E-18   1 7.370E-18   2 1.055E-17   3 1.190E-17   4 1.191E-17   5 1.124E-17
  6 1.032E-17   7 9.393E-18   8 8.545E-18   9 7.801E-18 10 7.156E-18 11 6.602E-18
.....................................................................

 42 4.528E-18 43 4.672E-18 44 4.826E-18 45 4.989E-18 46 5.158E-18 47 5.329E-18
 48 5.481E-18 49 5.524E-18
R_NU=49                 Z= 1  TE= 1.000E+04  NE= 1.000E+02  CASE=B
  0 2.812E-18   1 7.829E-18   2 1.121E-17   3 1.265E-17   4 1.266E-17   5 1.194E-17
.....................................................................

R_NU= 3                 Z= 1  TE= 1.000E+04  NE= 1.000E+02  CASE=B
  0 1.534E-14   1 3.726E-14   2 6.426E-14
R_NU= 2                 Z= 1  TE= 1.000E+04  NE= 1.000E+02  CASE=B
```

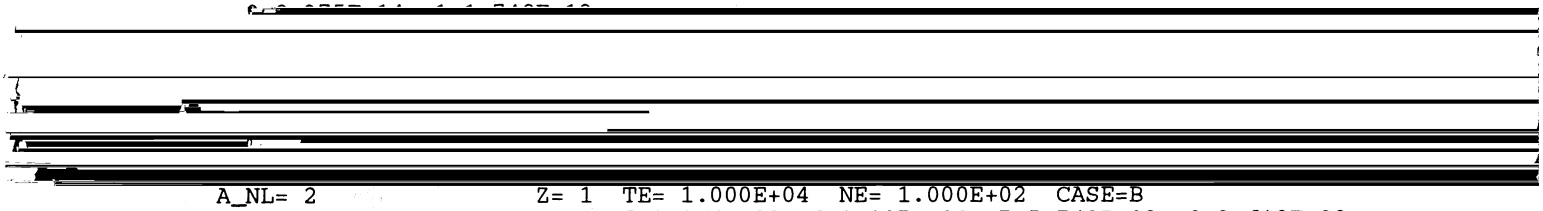

```
A_NL= 2                 Z= 1  TE= 1.000E+04  NE= 1.000E+02  CASE=B
  3 3.240E-07   4 5.672E-08   5 2.066E-08   6 1.007E-08   7 5.742E-09   8 3.612E-09
  9 2.431E-09 10 1.720E-09 11 1.264E-09 12 9.572E-10 13 7.432E-10 14 5.890E-10
.....................................................................

 39 2.578E-11 40 2.388E-11 41 2.217E-11 42 2.061E-11 43 1.920E-11 44 1.792E-11
 45 1.675E-11 46 1.567E-11 47 1.469E-11 48 1.379E-11 49 1.296E-11 50 1.219E-11
A_NL= 3                 Z= 1  TE= 1.000E+04  NE= 1.000E+02  CASE=B
  4 2.612E-13   5 5.584E-14   6 2.125E-14   7 1.059E-14   8 6.131E-15   9 3.906E-15
.....................................................................

A_NL=49                 Z= 1  TE= 1.000E+04  NE= 1.000E+02  CASE=B
 50 2.096E-08
B_NU=50                 Z= 1  TE= 1.000E+04  NE= 1.000E+02  CASE=B
  0 6.281E-01   1 5.940E-01   2 5.771E-01   3 6.293E-01   4 6.824E-01   5 7.253E-01
  6 7.581E-01   7 7.826E-01   8 8.008E-01   9 8.144E-01 10 8.245E-01 11 8.320E-01
.....................................................................

 42 8.381E-01 43 8.379E-01 44 8.377E-01 45 8.376E-01 46 8.374E-01 47 8.373E-01
 48 8.371E-01 49 8.369E-01
B_NU=49                 Z= 1  TE= 1.000E+04  NE= 1.000E+02  CASE=B
  0 6.264E-01   1 5.872E-01   2 5.664E-01   3 6.225E-01   4 6.796E-01   5 7.255E-01
.....................................................................

B_NU= 3                 Z= 1  TE= 1.000E+04  NE= 1.000E+02  CASE=B
  0 1.017E+00   1 2.317E-01   2 8.323E-02
B_NU= 2                 Z= 1  TE= 1.000E+04  NE= 1.000E+02  CASE=B
  0 4.569E+05   1 4.432E-03
BNS:                 Z= 1  TE= 1.000E+04  NE= 1.000E+02  CASE=B
  2 1.142E+05   3 2.365E-01   4 2.907E-01   5 3.819E-01   6 4.715E-01   7 5.480E-01
  8 6.101E-01   9 6.596E-01 10 6.988E-01 11 7.300E-01 12 7.548E-01 13 7.748E-01
.....................................................................

494 1.000E+00495 1.000E+00496 1.000E+00497 1.000E+00498 1.000E+00499 1.000E+00
500 1.000E+00
```

Figure 1. Structure of primary file **r1b0100.d**. The significance of the symbols is discussed in the text. Dotted lines indicate data removed to improve readability.

applications programs). Then come the emissivities for transitions from the upper state n_u, **E_NU** = n_u, preceded by the values of n_l in ascending order.

The effective recombination coefficients to state (n, l) are designated by **R_NU** = n, followed by the values of l in ascending order. The opacity factors for transitions from n_l to n_u are labelled by **A_NL** = n_l, and the entries are labelled with n_u in ascending order. Next come the departure coefficients $b(n, l)$, labelled by **B_NU** = n, with the entries identified by l in ascending order. The file is closed by the $b(n)$ following the symbol **BNS:**, with entries labelled by n.

With an interactive editor, one searches first for the desired value of N_e, then the identifier with the quantum number and finally the other quantum number. In designing an application program to use these files, it is useful to know that the material for each density occupies 1190 lines.

5 COMPRESSED INTENSITY FILES AND HANDLING PROGRAM

The secondary files containing emissivities and total recombination coefficients are sufficiently small that they can be stored in small computers and accessed interactively. The data set contains 16 files labelled **ezc.d**, in the same notation as above. Now results for all temperatures and densities appear in the same file.

The first line in each file gives the number of temperatures and the number of densities at which emissivities are tabulated. Then, for each pair of N_e and T_e, the emissivities are given together with the Case, the charge Z, the parameter n_c, and the maximum value n_{cut} of n contained in the table; in the present tables $n_{cut} = 25$, but this is not assumed in the interactive program. Then follows a linear array of emissivities for transitions from the upper level n_u to the lower level n_l, with n_u in descending order from n_{cut}, and n_l ascending from 1 to $n_u - 1$. In other words, the ordinal number in the array of the transition (n_u, n_l) is

$$k = n_l + (n_{cut} - n_u)(n_{cut} + n_u - 1)/2.$$

In Case B the emissivity for $(n_u, 1) = 0$ by definition, except for $n_u = 2$, where we have assumed that the Lyα escape probability is unity. For most purposes this provides the best approximation to the $n = 2$ populations (see Paper I), although the resulting Lyα emissivity is meaningless.

These files are accompanied by an interactive data server INTRAT. Upon calling INTRAT, cues are given for the ion charge and Case. The appropriate file is then loaded and a list of T_e and N_e is displayed. A cue is then given for the minimum density at which line ratios, emissivities or total recombination coefficients are to be displayed; the requested data are displayed at seven densities, starting with the lowest value equal to or greater than that specified, and for *all* available temperatures. Next, the user cues for the desired data type. If line ratios or emissivities are requested, the program then cues for the upper and lower quantum numbers of both transitions forming the ratio – the second pair specifying the 'reference' transition. If the quantum numbers of this reference transition are set to zero, then the emissivity of the transition specified by the first pair is given. Setting all four quantum numbers to zero is one way to end the program.

The requested line ratio, emissivity or total recombination coefficient is displayed as a table, with rows and columns corresponding to temperature and density, respectively. Cues are then given for *linear* or *logarithmic* interpolation in N_e and T_e, for resetting the minimum density, for entering a new set of transitions, or for exiting the program.

A two-dimensional Lagrange formula in the variables $T_e^{1/2}$ and ln N_e is used to interpolate either the tabulated quantity or its logarithm. The latter choice seems to be preferable, and is indeed necessary in interpolating emissivities and recombination coefficients. Equal numbers of points are used in each variable and interpolations with up to five values of the order are made simultaneously. This allows the user to judge the degree of reliability of the interpolation. The program returns interpolates of orders 2, 3, 4, and 5. The same choice of options as above is then cued. As the specified quantity is computed at *all* values of N_e and T_e, and not just those displayed on the screen, the interpolation loses accuracy only near the edge of the *complete* table. Moreover, the interpolation facility can be used for values not currently displayed.

Finally, all tables and interpolates produced during the interactive session are stored in file **intratzc.d** for printing; here **z** and **c** are again the charge and Case. The code contains extensive internal documentation.

6 APPLICABILITY OF THE DATA

In the application of the data presented here, several restrictions must be kept in mind. Obviously the transitions must be optically thin, which can be checked with the opacity factor. The degree of ionization and the optical depth in the Lyα transition must satisfy the inequalities given in Papers I and II, to ensure that collisions from the ground and first excited states do not contribute to the populations of higher states. These effects cannot be included without introducing additional parameters and are especially important for high densities.

Data for hydrogenic ions may also be applied to transitions in non-hydrogenic systems in certain circumstances. The states involved must be approximately hydrogenic in nature; a transition between states of high principal quantum number, for example, where the nearly hydrogenic high-l-substates dominate the emissivity. The principal uncertainty in using hydrogenic data for such transitions is in the neglect of dielectronic recombination. The low-temperature dielectronic process described by Storey (1981) usually arises through recombinations directly to relatively low-lying states, whereas the high-temperature process described by Burgess (1964) populates states of high principal quantum number. As the data given here are applicable only for relatively highly excited states in non-hydrogenic ions, care should be taken that the temperature is below that at which high-temperature dielectronic recombination is important for that ion. Threshold temperatures for this process are given for ions of C, N and O by Nussbaumer & Storey (1983). Note also that, except for helium-like ions, the ground state of a non-hydrogenic system will not contain $n = 1$ orbitals, so that Case B data will be appropriate rather than Case A data.

In some cases, the l components of a transition in a non-hydrogenic ion may be spectrally resolved, but the states may be approximately hydrogenic; the 5g–4f transition in C II, for example. Bearing in mind the uncertainties discussed above,

emissivities for this transition may be calculated from the tabulated departure coefficient for the $Z = 2$ 5g state and the appropriate transition probability. Subroutines for the evaluation of these probabilities in hydrogenic ions are available (Storey & Hummer 1991).

For more complex ions, a further division into multiplet structure may be needed; the $(^2P^o)5g$–$(^2P^o)4f$ transitions in N II, for example. Such a division, using standard tables of multiplet strengths in LS-coupling may be unreliable. The states of higher l for which the hydrogenic data are valid are just those for which the assumption of LS-coupling is *least* likely to be justified, so evidence should be sought, from energy-level tables for example, that the assumption of LS-coupling is justified.

7 ACCESS TO MACHINE-READABLE DATA FILES AND DATA SERVER

For details on how to obtain the data and program described above, please contact the NSSDC Coordinated Request and User Support Office electronically at REQUEST@NSSDCA.GSFC.NASA.GOV (Internet), NSSDCA::REQUEST (NSI-DECnet); by telephone at (301) 286-6695; or write to the Coordinated Request and User Support Office, Code 633.4, Goddard Space Flight Center, Greenbelt, MD 20771, USA. This material may also be obtained from the Centre de Données Astronomique de Strasbourg, 11 Rue de l'Université, F-67000 Strasbourg, France. The data files can be accessed directly by anonymous ftp to cdsarc.u-strasbg.fr, where they can be found in directory /pub/cat/VI/64.

REFERENCES

Baker J. G., Menzel D. H., 1938, ApJ, 88, 52
Burgess A., 1964, ApJ, 139, 776
Hummer D. G., Storey P. J., 1987, MNRAS, 224, 801 (Paper I)
Hummer D. G., Storey P. J., 1992, MNRAS, 254, 277 (Paper III)
Nussbaumer H., Storey P. J., 1983, A&A, 126, 75
Storey P. J., 1981, MNRAS, 195, 27P
Storey P. J., Hummer D. G., 1988, MNRAS, 231, 1139 (Paper II)
Storey P. J., Hummer D. G., 1991, Comput. Phys. Commun., 66, 129